Zeeman splitting measurements of magnetic fields in iodine plasma

Thomas E. Steinberger,[a] Mikal T. Dufor, Derek S. Thompson, and Earl E. Scime
Department of Physics, West Virginia University, Morgantown, West Virginia 26506, USA

(Presented 16 April 2018; received 4 May 2018; accepted 18 June 2018;
published online 5 October 2018)

Iodine is an attractive propellant for next generation ion thrusters. Laser induced fluorescence (LIF) is widely used with other propellant species as a non-perturbative technique for measuring flow for thruster prediction models. We apply LIF methods recently demonstrated for singly-ionized iodine to a magnetized plasma environment similar to those found in ion thrusters and in magnetically confined laboratory plasmas. We demonstrate the feasibility of remotely determining the local magnetic field from the Zeeman effect-split spectrum of I^+. *Published by AIP Publishing.*
https://doi.org/10.1063/1.5038641

I. INTRODUCTION

Iodine is an attractive alternative propellant for plasma thrusters, which have traditionally relied on xenon fuel. Both atoms have similar low ionization potentials and are nearly equal in mass. Storage of iodine in solid form at room temperature eliminates many of the mechanical challenges of gaseous propellants like xenon.[1–7] A recently demonstrated laser induced fluorescence (LIF) method for interrogating singly ionized atomic iodine (I-II) provides a non-perturbative diagnostic measurement of the ion velocity distribution function (IVDF) in an iodine plasma.[8]

Because a magnetic field splits electronic states into multiple energy levels (Zeeman splitting), LIF measurements of the splitting of I-II lines also provide a potential method of measuring the local magnetic field strength inside magnetized plasma thrusters and other magnetized plasma sources. For weak to moderate magnetic field strengths, each electronic state splits into $2J + 1$ components according to

$$\Delta E = \mu_B g m_J B_{\text{ext}}, \tag{1}$$

where J is the sum of the orbital angular momentum and the spin for the electronic state, μ_B is the Bohr magneton, g is the Landé g factor for the unsplit state, m_J is the magnetic quantum number of the unsplit state, and B_{ext} is the external magnetic field. The hyperfine structure of the I-II LIF transition sequence is substantial,[8] and even for weak to moderate magnetic fields, Zeeman splitting is expected to significantly modify the measured absorption spectrum of I-II.

The aim of this work is to quantify the Zeeman splitting of the I-II LIF transition to establish a diagnostic tool for magnetic field measurements in iodine plasma systems with limited diagnostic access. Here we provide first measurements of the Zeeman splitting of clearly identifiable clusters of transitions in LIF iodine ion spectra and determine the scaling of the Zeeman splitting of the $^5D_4^o - {}^5P_3$ transition for I-II.

Note: Paper published as part of the Proceedings of the 22nd Topical Conference on High-Temperature Plasma Diagnostics, San Diego, California, April 2018.

[a]Author to whom correspondence should be addressed: testeinberger@mix.wvu.edu

II. EXPERIMENT

A. LIF scheme

The LIF scheme used here was first proposed by Hargus *et al.* and briefly investigated using passive emission spectroscopy.[1] Figure 1 shows a partial Grotrian diagram illustrating the pump and fluorescent transitions. The $^5D_4^o$ metastable state is excited to the $^5P_3$ state by 696.0694 (vac.) nm light.[8] The $^5P_3$ state then relaxes to the $^5S_2^o$ state, emitting a photon at 516.264 nm (vac.).[9]

The transition used for this work has significant hyperfine splitting from nuclear magnetic dipole and electric quadrupole moments. A detailed investigation of the hyperfine splitting is provided by others[1,8] and is only briefly mentioned here. The energy shift of hyperfine splitting is calculated by

$$\Delta E = \frac{A}{2}C + \frac{B}{4}\frac{\frac{3}{2}C(C+1) - 2I(I+1)J(J+1)}{I(2I-1)J(2J-1)}, \tag{2}$$

where A is the nuclear magnetic dipole coupling coefficient, B is the electric quadrupole coupling coefficient, $C = F(F+1) - I(I+1) - J(J-1)$, F is the total angular momentum of the nucleus-electron system, I is the nuclear spin, and J is the total electric angular momentum.[10] The pump transition yields 15 hyperfine transitions, with 11 likely to be resolvable.[1,8]

The magnetic dipole and electric quadrupole coupling coefficients must be known to predict the energy shift due to hyperfine splitting. These coefficients are not currently known, although Steinberger and Scime[8] have determined bounds for the magnetic dipole coefficient.

B. Zeeman splitting of I-II

The pump transition is further broadened by the Zeeman effect. For large enough magnetic fields—$\gtrsim$100 mT for this work—the Zeeman splitting is comparable to the hyperfine structure. For even stronger fields, the applied magnetic field sufficiently decouples the total electronic angular momentum, J, from the nuclear spin, I.[11] In this case, the energy shifts are more appropriately described by the hyperfine Paschen-Back (HPB) effect, which is analogous to the regular Paschen-Back effect when an ambient magnetic field decouples the electron

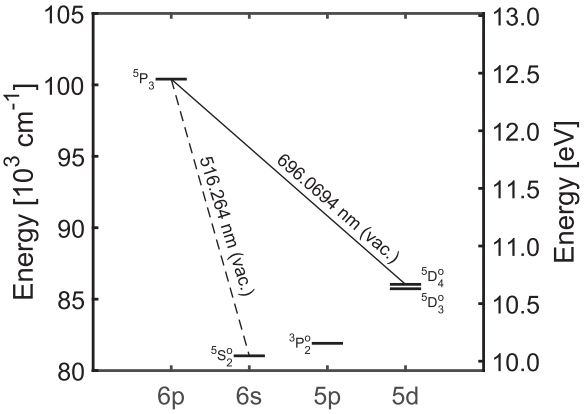

FIG. 1. Partial Grotrian diagram for the LIF scheme used in this work. The pump transition is excited by a 696.0694 nm (vac.) photon and a 516.264 nm (vac.) photon is collected.

spin from the orbital angular momentum.[12] The frequency shifts of the Zeeman-hyperfine transitions from rest frequency are then approximated by

$$\Delta\nu \approx (g_J m_J \mu_B + g_I m_I \mu_N) B_{ext} h^{-1}, \quad (3)$$

where g_J and g_I are the Landé g factors for the total electronic angular momentum and nuclear spin respectively; μ_N is the nuclear magneton; m_J and m_I are the respective magnetic quantum numbers for a state with a given total electronic angular momentum, J, and nuclear spin, I; and h is Planck's constant.[12]

For dipole transitions, the nuclear spin is unaffected, therefore the selection rules for a transition in the HPB regime are

$$\Delta m_I = 0, \quad (4)$$

$$\Delta m_J = 0, \pm 1, \quad (5)$$

$$\Delta F = 0, \pm 1 \quad (6)$$

except if $m_J = m'_J = 0$ or $F = F' = 0$. Unprimed quantities indicate initial transition states and primed quantities represent final transition states.[11] Because the magnetic dipole and electric quadrupole coupling coefficients required to calculate the hyperfine structure of the pump transition are still unknown, it is not yet possible to calculate the combined hyperfine-Zeeman energy shifts. It was hoped that the Zeeman splitting of this transition would be large enough to isolate a single hyperfine transition and thereby enable the direct measurement of the magnetic dipole and electric quadrupole coefficients. However, single transition features were not resolvable due to the added complexity of the atomic structure and insufficiently strong magnetic field. Fortunately, direct measurements of the spectra as a function of ambient magnetic field strength are sufficient to develop the diagnostic method.

C. Experimental apparatus

The plasma source used in this work has been described elsewhere[1,8,13] and is only briefly described here. Crystalline iodine is sealed inside an Opthos Instruments, Inc. vapor cell

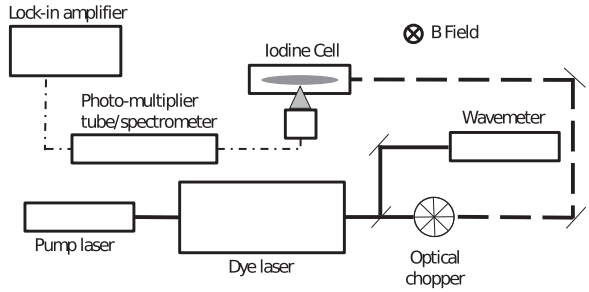

FIG. 2. Optical layout of I-II LIF experiment.

at $<10^{-4}$ Torr. The cell is placed partially inside an Evenson microwave cavity that is driven at 2.45 GHz. Iodine partial pressure is controlled by circulating a chilled water-ethylene glycol (EG) solution through a chilling finger extending off the iodine cell. The coolant is chilled using a Polyscience PD07R-40 that has an operating range of −20 to 100 °C. The dependence of iodine partial pressure, P, on chilling finger temperature, T_{CF}, was investigated by Kono and Hattori[14] in a similar source and was found to be

$$\log_{10} P = 18.8 - \frac{3954}{T_{CF}} + 0.000\,44\,T_{CF} - 2.98 \log_{10} T_{CF}, \quad (7)$$

where T_{CF} is in kelvin and P is in Torr.

Figure 2 shows the optical configuration used in this work. A Sirah Matisse dye-ring laser is pumped by a Spectra-physics Millenia Pro laser at 532 nm. The laser output is monitored by a Bristol 621 wavelength meter that is accurate to ±0.2 pm.

Fluorescent emission is collected perpendicularly to the axis of the iodine cell by a 1 mm core multi-mode fiber coupled to the entrance slit of a McPherson Model 209 Czerny-Turner scanning monochromator. The spectrometer effectively acts as a ±5 nm bandpass filter. A Hamamatsu 10493 photo-multiplier tube is fixed to the exit slit of the spectrometer and amplifies the fluorescent emission. Signal is distinguished from spontaneous emission by a Stanford Research SR830 lock-in amplifier referenced to a 5 kHz mechanical chopper.

Two permanent magnets are placed above and below the cell, creating a magnetic field perpendicular to the laser injection axis (into the page in Fig. 2). The distance between the magnets is varied to produce $B_{ext} = 25$–300 mT with $\delta B_{ext}/B_{ext} \leq 4\%$.

III. RESULTS

A. Zeeman shift of $\sigma_\pm$ clusters

Figure 3 shows the hyperfine-broadened, Zeeman-split line shape of the pump transition at several magnetic field strengths. Injecting laser light with its axis of polarization perpendicular to the magnetic fields isolates the $\sigma_\pm$ ($\Delta m_J = \pm 1$) components and suppresses the π ($\Delta m_J = 0$) components from the Zeeman-split spectrum. An approximately 25 GHz sweep is sufficient to capture the Zeeman shift of the most prominent $\sigma_\pm$ components for each IVDF.

For $B \gtrsim 100$ mT, the two dominant $\sigma_\pm$ clusters are easily resolved. The frequency shift of each $\sigma_\pm$ component, $\Delta\nu$, from the rest frequency is linearly proportional to the ambient

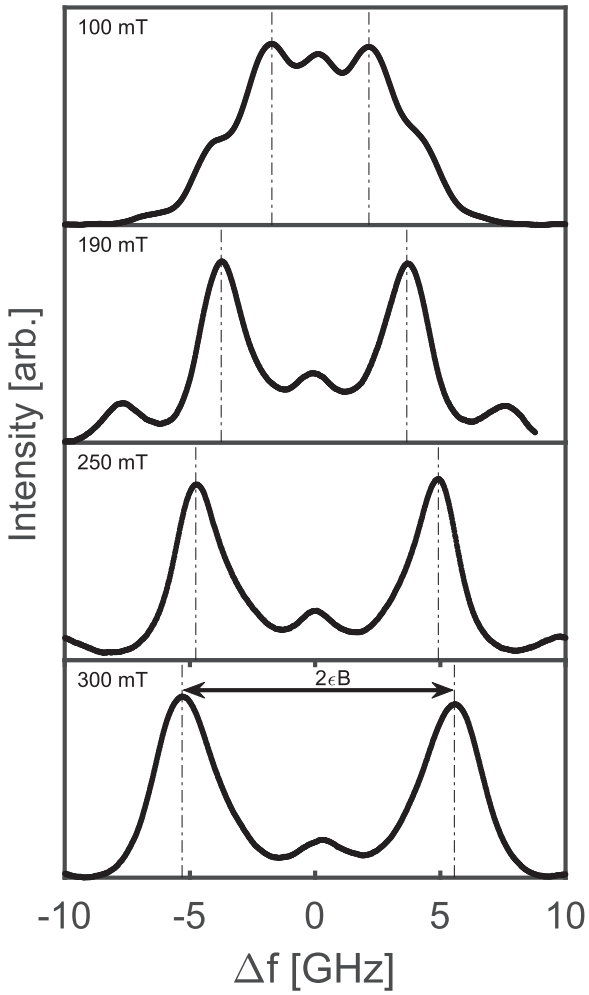

FIG. 3. Zeeman shift of the $\sigma_{\pm}$ components for an ambient magnetic fields $\gtrsim$100 mT.

magnetic field: $\Delta\nu = \epsilon B_{\text{ext}}$. Figure 4 shows the $\Delta\nu$ dependence on magnetic field. The Zeeman shift coefficient ϵ is determined from the slope of a linear fit to the data in Fig. 4 and is found to be 19 ± 1 MHz/mT ($\delta\epsilon/\epsilon \approx 6\%$). The uncertainty is determined from the uncertainty in the laser frequency (i.e., shot-to-shot variation, wavemeter accuracy, and sampling rate), $\delta(\Delta\nu)/\Delta\nu \approx 5\%$, the uncertainty in the Hall probe measurement of B_{ext}, $\delta B_{\text{ext}}/B_{\text{ext}} \approx 4\%$, and the uncertainty in ϵ from a linear fit, $(\delta\epsilon/\epsilon)_{\text{fit}} \approx 1\%$. The uncertainties are added in quadrature.

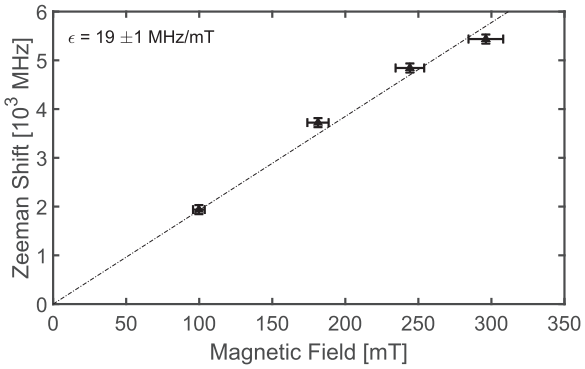

FIG. 4. Frequency shift of the $\sigma_{\pm}$ components for $B_{\text{ext}} \geq 100$ mT.

Reversing the process, the local perpendicular magnetic field is determined from the measured $\sigma_{\pm}$ shifts.[15] The uncertainty in the measured field $\delta B_{\text{meas}}/B_{\text{meas}}$ is the quadrature sum of the uncertainties in the Zeeman shift coefficient ϵ and the Zeeman shift $\Delta\nu$. A conservative upper bound on the uncertainty is $\delta B_{\text{meas}}/B_{\text{meas}} \approx 8\%$. For $B_{\text{ext}} \lesssim 100$ mT, the $\sigma_{\pm}$ clusters overlap and weaker fields cannot be determined by a single spectrum. The range of resolvable magnetic field strengths can be extended to weaker fields by inserting a quarter-wave plate between the linear polarizer and the plasma, circularly polarizing the laser, and isolating a single σ peak (i.e. σ_+ or σ_-). The quarter-wave plate is then rotated so that the opposite polarization occurs. The peak separation is obtained by overlaying the two isolated spectra. The single peak shift measurement method is constrained by the uncertainty in the frequency measurement, $\delta\nu$. Using $\delta\nu$ = 200 MHz as a conservative theoretical minimum resolvable frequency shift and ϵ = 19 MHz/mT, we predict that field strengths as low as $B_{\text{ext}} \approx 10$ mT are resolvable. Isolation of a single σ peak to perform high resolution LIF measurements of flow and temperature is a common diagnostic technique.[16]

IV. CONCLUSION

We have demonstrated a new diagnostic for non-perturbatively measuring iodine IVDFs and local magnetic field strength when an external field is applied. Combined with new optical techniques that permit LIF measurements using only a single line-of-sight,[17] this method has the potential to provide magnetic field measurements deep inside the channels of cylindrically symmetric thrusters such as Hall thrusters operating in iodine where there is little optical access and no access for physical probes. The Zeeman shift of each $\sigma_{\pm}$ component for $B_{\text{ext}} > 100$ mT is 19 ± 1 MHz/mT, resulting in an uncertainty for magnetic field determination of $\delta B_{\text{meas}}/B_{\text{meas}} \leq 8\%$.

ACKNOWLEDGMENTS

We would like to thank Dr. William Hargus, Jr. at the Edwards Air Force Research Laboratory for providing many pieces of equipment used in this work. This work was supported by the U.S. National Science Foundation Grant Nos. PHY-1360278 and PHY-0918526.

[1] W. Hargus, J. Lubkeman, K. Remy, and A. Gonzales, AIAA Paper 2012-4316, July 2012.
[2] A. Hiller, "Revolutionizing space propulsion through the characterization of iodine as fuel for Hall-effect thrusters," M.Sc. thesis, Air Force Institute of Technology, Wright Patterson Air Force Base, 2011.
[3] R. Dressler, Y.-H. Chiu, and D. Levandier, AIAA Paper 2000-0602, January 2000.
[4] J. Szabo, B. Pote, S. Paintal, M. Robin, A. Hiller, R. D. Branam, and R. E. Huffman, J. Propul. Power **28**, 848 (2012).
[5] J. Szabo, M. Robin, S. Paital, B. Pote, V. Hruby, and C. Freeman, in 33rd International Electric Propulsion Conference, October 2013, IEPC Paper 2013-311.
[6] J. A. Linnell and A. D. Gallimore, J. Propul. Power **22**, 1402 (2006).
[7] O. Tverdokhlebov and A. Semenkin, AIAA Paper 2001-3350, July 2001.
[8] T. Steinberger and E. Scime, J. Propul. Power **34**, 1235 (2018).

[9]W. C. Martin and C. H. Corliss, J. Res. Natl. Bur. Stand., Sect. A **64A**, 443 (1960).
[10]R. D. Cowan, "External fields and nuclear effects," in *The Theory of Atomic Structure and Spectra*, 1st ed. (University of California Press, Berkeley, 1981), Chap. 17, pp. 506–511.
[11]H. Kuhn, "Hyperfine structure and isotope shift," in *Atomic Spectra*, 2nd ed. (Academic Press, New York, 1962), Chap. 6, pp. 354–360.
[12]M. A. Zentiel, R. Andrews, L. Weller, S. Knappe, C. S. Adams, and I. G. Hughes, J. Phys. B: At., Mol. Opt. Phys. **47**, 075005 (2014).
[13]F. Fehsenfeld, K. Evenson, and H. Broida, Rev. Sci. Instrum. **36**, 294 (1964).
[14]A. Kono and S. Hattori, J. Opt. Soc. Am. **69**, 253 (1978).
[15]D. S. Thompson, T. E. Steinberger, A. M. Keesee, and E. E. Scime, Plasma Sources Sci. Technol. **27**, 065007 (2018).
[16]D. S. Thompson, R. Agnello, I. Furno, A. Howling, R. Jacquier, G. Plyushchev, and E. E. Scime, Phys. Plasmas **24**, 063517 (2017).
[17]D. S. Thompson, M. F. Henriquez, and E. Scime, Rev. Sci. Instrum. **88**, 103506 (2017).